ГОДИШНИК НА СОФИЙСКИЯ УНИВЕРСИТЕТ „СВ. КЛИМЕНТ ОХРИДСКИ“
ФИЗИЧЕСКИ ФАКУЛТЕТ, ЮБИЛЕЙНО ИЗДАНИЕ
130 ГОДИНИ СОФИЙСКИ УНИВЕРСИТЕТ
и 55 ГОДИНИ ФИЗИЧЕСКИ ФАКУЛТЕТ
„Нови научни постижения и направления във Физически факултет“

ANNUAL OF SOFIA UNIVERSITY “ST. KLIMENT OHRIDSKI”
FACULTY OF PHYSICS, JUBILEE EDITION
130th ANNIVERSARY OF SOFIA UNIVERSITY
and 55th ANNIVERSARY OF FACULTY OF PHYSICS
“*New scientific achievements and directions in the Faculty of Physics*”

SEISMIC ACTIVITY OF SOUTH SHETLAND ISLANDS: RESULTS FROM EXPOATATION OF FIRST BULGARIAN BROAD BAND SEISMIC STATION IN ANTARCTICA

L. DIMITROVA[1], G. GEORGIEVA[2], P. RAYKOVA[1], V. PROTOPOPOVA[1], I. ALEKSANDROVA[1], M. POPOVA[1], D. DIMITROV[1], V. GOUREV[3],R. RAYKOVA[2], D. SOLAKOV[1]

[1] National Institute of Geophysics, Geodesy and Geography, BAS
[2] Department of Meteorology and Geophysics, Faculty of Physics, Sofia University
[3] Department of Atomic Physics, Faculty of Physics, Sofia University

Л. Димитрова, Г. Георгиева, П. Райкова, В. Протопопова, И. Александрова, М. Попова, Д. Димитров, В. Гурев, Р. Райкова, Д. Солаков. СЕИЗМИЧНА АКТИВНОСТ НА ЮЖНОШЕТЛАНДСКИТЕ ОСТРОВИ: РЕЗУЛТАТИ ОТ РАБОТАТА НА ПЪРВАТА БЪЛГАРСКА ШИРОКОЛЕНТОВА СЕИЗМИЧНА СТАНЦИЯ В АНТАРКТИКА

Сеизмична станция LIVV е инсталирана в рамките на три антарктически експедиции в периода 2015 г. до 2018 г. През първия период на работа на станцията – астралното лято на 2015–2016 г., са регистрирани около 200 земетресения. Оценката за работата на сеизмичната апаратура показва възможността на станция LIVV да регистрира сеизмични събития с различен произход. За локализиране на регистрираните сеизмични събития са използвани два метода. Единят се основава на метода на Голицин и формулите на Vincenty, а другият е чрез софтуера Dhypo, като са използвани различни скоростни модели и фази от две сеизмични станции от Аржентино-Италианската мрежа (AI) и четири испански станции, разположени на о-в Десепшън.

For contact: Gergana Georgieva, Department of Meteorology and Geophysics, Faculty of Physics, Sofia University „St. Kliment Ohridski“, 5 James Bourchier Blvd, 1164 Sofia, Phone: +359 887 060 397, E-mail: ggeorgieva@phys.uni-sofia.bg

Seismic station LIVV is deployed within three Antarctic expeditions from 2015 to 2018. During the first deployment period in astral summer 2015–2016 about 200 earthquakes were recorded. The estimated performance of the seismic equipment shows off the capabilities of the LIVV station to registered seismic events with different nature. Two methods for earthquakes localization are used. One is based on Golitsyn's method and Vincenty formulae and other is using DHypo software with different velocity models and phases from two Argentinean-Italian (AI) stations and four Spanish stations deployed on Deception Island Volcano.

Keywords: Antarctica seismicity, Bulgarian Antarctic seismic station, Golitsyn's method
PACS numbers: 91.30.Dk, 91.30.P*x*, 93.30.Ca, 91.10.Kg, 93.85.Bc

1. INTRODUCTION

Until the end of 1950s seismicity of Antarctic region was connected only with the active volcanoes – Mount Erebus and Deception Island [1, 2], and the Antarctic continent was thought as less seismic than the others continents. The low seismicity was difficult to verify due to the absence of seismic stations in the region. Even after the installation of first couple of seismic stations no earthquakes were reported within years [3]. However, with the time it was understood that this part of the globe is a very complex geodynamic system combining subduction zone, rifting and spreading zones and magmatic activity. Any of these zones should be manifested with high seismicity. One great earthquake with magnitude $Ms = 8.0$ struck the Balleny Islands region on March 25, 1998. This earthquake is the largest one ever recorded in the Antarctic region [3]. The first felt shock in the Antarctica was the magnitude 4.7, December 4, 1967 earthquake accompanied by the volcanic eruption at Deception Island [4]. First recorded earthquake located in Antarctica occurred in 1982.

Increasing number of seismic stations installed in Antarctica took advantage a big amount of low magnitude earthquakes to be detected even on the Antarctic continent [5–7].

The region of South Shetland Islands is one of the most active in Antarctica. Recently more and more scientific institutions have projects to study various aspects of seismicity of the region. Most of the seismic stations are situated on King George Island where many countries have bases. Several studies including Ocean Bottom Stations (OBS) deployment and deep seismic profiling [8] were conducted in Bransfield strait and Drake passage. Due to volcanic activity of Deception volcano [9, 10] seismic array was installed on the island [11]. In 2014 an increase of seismic activity on Livingston Island was observed from Almendros et al. [12]. It remains high until the end of austral summer in 2016 [13] and in 2018 few events from this group are registered.

Seismic station on Livingston Island was deployed in 2008, during the Spanish polar expedition near to the Spanish base – Juan Carlos I, neighboring the Bulgarian Base [14]. Registration of seismic events was done also near Bulgarian Base during the astral summer 2000–2001 [15] using 4.5 Hz short-period geophone and digital autonomous device set up in triggered mode. Bulgarian broadband seismological station LIVV is installed on 19.12.2015 near the Bulgarian Antarctic Base „St. Kliment Ohridski“ [13]. From 2015 it became operational for the astral summers.

After the three seasons of registration more than 10000 seismic events were identified. The identification of the recorded events was performed by visual scanning of the raw records. We have distinguished two main types of events: ice-generated seismic events and tectonic earthquakes. In the paper we present a study of the seismicity of the Livingston Island region on the base of registered by LIVV station tectonic events during the first operating period in 2015–2016.

2. GEOLOGY AND SEISMICITY OF SOUTH SHETLAND ISLANDS

Livingston Island is second largest from South Shetland Islands archipelago. This region represents a continental fragment [16, 17] situated in the transition zone between Drake (Phoenix) plate in the North and Antarctic plate in the South. The geological setting of the region is considered to be unique because of its current transformation from subduction to spreading zone. Geological history of the region consists of three main stages – pre-subduction, main subduction and extensional stage [18]. The extensional stage is considered as a typical for opening of the Bransfield Strait Rift [19, 20]. This complex geodynamics is reflected by the presence of active volcanoes in the present [17] and shallow and intermediate seismicity. Even the Bransfield strait is an active rifting zone the subduction is still active along the South Shetland Trench. It is considered as last active part of a subduction zone from that was once extended all along the western margin of the Antarctic Peninsula [21]. The main tectonic units of Antarctic Peninsula and Scotia Sea are given on fig. 1.

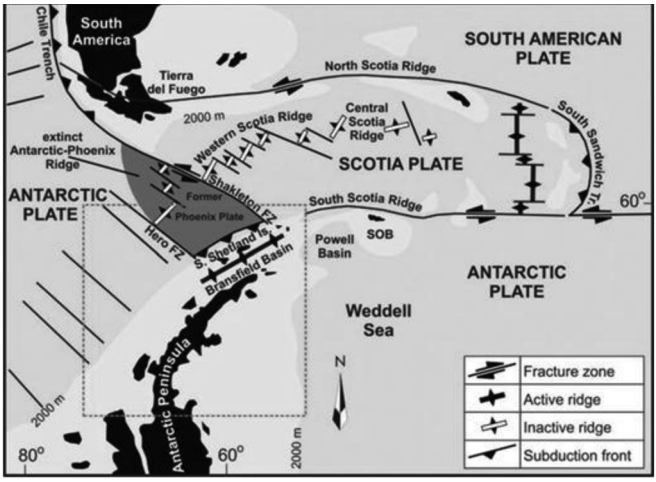

Fig. 1. Main tectonic units of Antarctic Peninsula and Scotia Sea [22]

3. EQUIPMENT DEPLOYMENT AND DATA AVAILABILITY

Station LIVV (62°38′11″ S, 60°20′89″ W) is situated on Livingston Island close to the calving zone of Perunika glacier and 1 km away from Bulgarian Antarctic Base „St. Kliment Ohridski" (fig. 2).

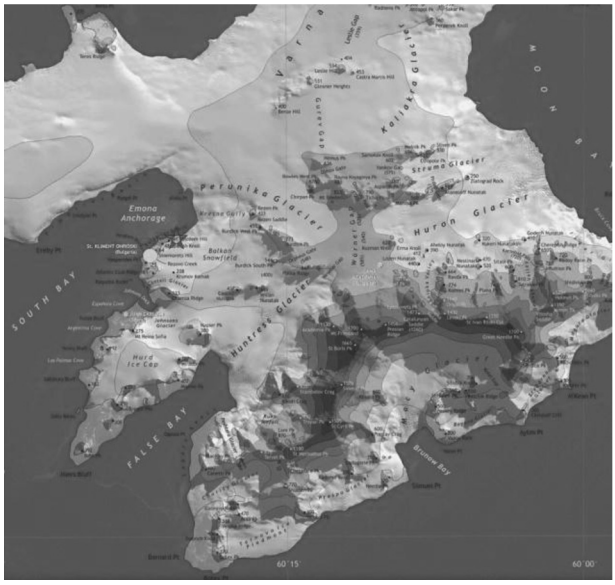

Fig. 2. Bulgarian Antarctic Base „St. Kliment Ohridski" on Livingston Island marked with yellow circle and LIVV Station – red star [23]

The seismological equipment comprised of a broad band (BB) and a short period (SP) seismometers and a 24 bit Digital Acquisition System (DAS) with GPS timing and two 4GB internal memory cards. Both seismometers were installed on a concrete pillar previously constructed on an outcrop (fig. 3). Seismometers were oriented according to the geographic North – a correction was made for the declination of 12°. Isolation cover was mounted over the sensors which ensured stable environment during the deployment period.

Data were recorded continuously at 100 Hz sample rate on the memory cards. At the beginning, the electric power was supplied by batteries which periodically were recharged in the Base. This caused small interruptions in the data recording during the battery change. Two weeks later a solar panel was installed at the site and uninterpretable power supply of the equipment was ensured.

Fig. 3. Seismological equipment installed on the pillar and solar panel

The first operational season of the LIVV station was 73 days long until 25.02.2016 when the 24th Bulgarian Antarctic Expedition finished. Figure 4 represents the data availability during the operational period of the station. The hours of the day and the days of the years are placed respectively on the vertical and horizontal axes. It is visible that there are no gaps in the data during the second half of the period when the solar panel went in operation.

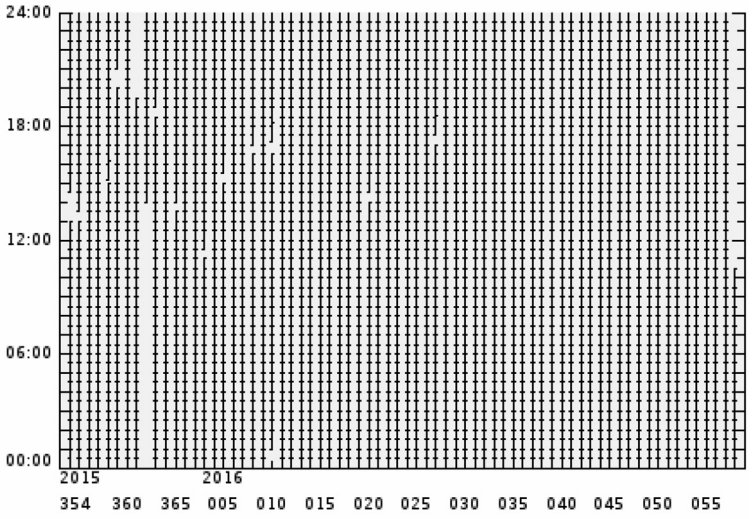

Fig. 4. Data availability during the deployment period of 73 days in the season 2015-2016

4. SEISMIC STATION LIVV PERFORMANCE

Ambient noise level has the greatest impact on the recording capabilities of the seismic station. We applied the Method of McNamara and Buland [24] to estimate Power Spectral Density (PSD) and Probability Density Function (PDF) of the ambient noise recorded by the LIVV station and assessed the ability of the station to register local and regional earthquakes and ice quakes. The seismic noise is produced mainly by natural phenomena due to the lack of human being action on the Island. In this aspect the Livingston Island is perfect laboratory to study and understand geodynamic behavior of the Earth.

Distribution of PSD and PDF for the three working months is given in the figure 5 together with the Low and High Noise Models (NLNM, NHNM [25]. For the periods of microseisms (periods from 5s to 8s) the PSD curve with highest level of probability extends close but not exceeds the NHNM (fig. 5). This is typical behavior of stations worldwide situated close to the cost line. On the other hand, the site is located on the closed bay banks, which freeze in winter. The ice cover attenuates the ocean waves and the expected level of microseisms in winter won't to be higher than the estimated values. For the periods below 5 s the highest probability PSD curve gradually moves away from the NHNM curve and the difference between the two curves reaches as many as 55 dB at the lowest periods (0.02s).

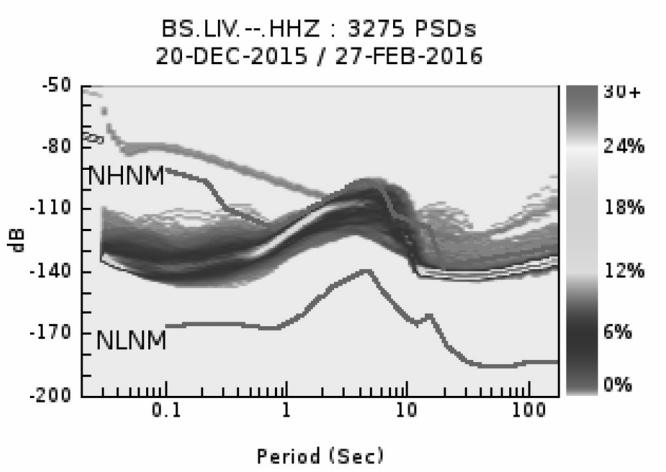

Fig. 5. Distribution of PSD and PDF of the ambient noise for the three working months together with the Low and High Noise Models (NLNM and NHNM)

The noise level for the highest frequencies (lowest periods) is affected mainly by weather conditions. Figure 6a represents the distribution of PSD of the noise during the strong wind with speed around 30m/s and figure 6b shows the noise level within a relatively quiet day (maximum wind speed is 8m/s). The mode PSD curve in fig. 6a reaches -110 dB at the period of 0.02s and it is situated of 30 dB below the NHNM curve. Figure 6b shows that the PSD curve is situated quite far from NHNM curve. Taking into account the distribution of PSD and PDF (fig. 5, fig. 6a and fig. 6b); it can be assumed that the magnitude threshold for local and regional earthquakes is about 1.

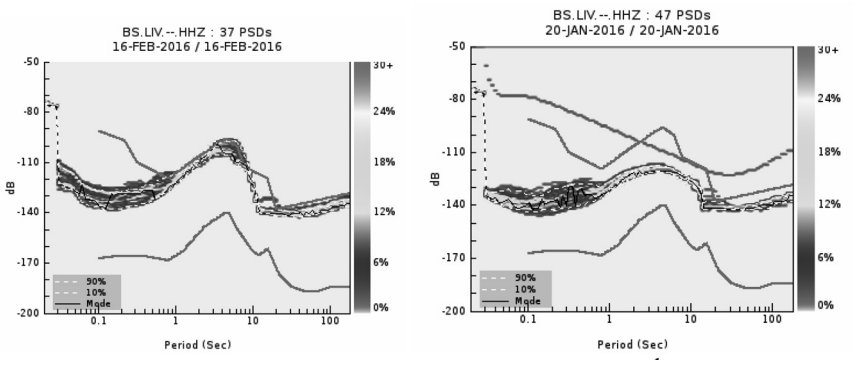

a b

Fig. 6. Distribution of the PSD of the noise during the strong wind (a); distribution of the PSD of the noise during the quiet day (b)

5. METHOD FOR LOCALIZATION OF EVENTS

5.1. PRELIMINARY PREPARATION OF DATA

About 200 events were categorized as local and regional earthquakes. We separated these events in three main groups using the time difference of P and S onsets (*Ts-p*) as follow:

1. T1 group – earthquakes with time difference *Ts-p* = 5s – 136 events;

2. T2 group – contains the earthquakes with time difference 5s < *Ts-p* < 30s – 25 events;

3. T3 group – recorded earthquakes with *Ts-p* > 30s were classified as regional or teleseismic events – 39 events.

Next attempt for events identification was looking for earthquakes in the region of the South Shetland Islands listed in the bulletins of the International Data Centers. No event located in the interested region during the deployment period (2015–2016) of the LIVV station was found. We suggest that the main reasons for lack of such information are small number of seismic stations in the region, low magnitude of the recorded earthquakes and short deployment period of LIVV station.

In addition, we used data recorded by permanent stations deployed in the region of Livingston Island. Continuous data of Argentinean–Italian (AI) Network [26] for the period December 2015–March 2016 were downloaded from the Incorporated Research Institutions for Seismology (IRIS) web site [27]. Data for the cited period of Spanish stations BASE, OBS, C70 and CHI were provided by Spanish colleagues. The stations are deployed at Deception Island Volcano [11].

Seismic phases for several earthquakes were picked as a result from visual scanning of data from AI and Spanish stations. These phases could be associated to events recorded by LIVV station (from T1 and T2 groups). In order to localize the most part of the earthquakes from the both groups two approaches were applied – single station method and standard minimization procedures.

5.2. SINGLE STATION METHOD

This method developed by Golitsyn [28] is based on analysis of the seismic signals recorded at one three-component seismic station. Distance to the earthquake's epicenter is computed from the difference between arrival times of P- and S-waves and travel-time tables. Velocity model for the Back arc region of South Shetland Islands limited up to 70 km depth [10] was used to compute the travel time table.

The back azimuth of the epicenter is computed by eq. 1:

$$\mathrm{tg}\alpha = Ae/An \tag{1}$$

where *Ae* is the amplitude of *P*-phase, registered on E-W component of the seismogram, *An* is P-phase amplitude from N-S component, and α is the back

azimuth (*BAZ*) of the earthquake. Both amplitudes are measured positive or negative. The sign of P-phase from vertical component estimates the real back azimuth according the following rule (Table 1) [29].

Table 1

	An	*Ae*	*Az*
$BAZ = \alpha$	+	+	–
	–	–	+
$BAZ = 180 - \alpha$	+	–	+
	–	+	–
$BAZ = 180 + \alpha$	+	+	+
	–	–	–
$BAZ = 360 - \alpha$	–	+	+
	+	–	–

Region of South Shetland Islands is situated quite close to the pole. This is a challenge finding good algorithm to compute geographic coordinates of epicenters. First approach to calculate earthquake locations on the base of Golitsyn formulae was presented in [13]. Later we found out that lots of uncertainties were generated applying this formulae earthquake's locations in the studied region. Then several algorithms were tested in order to find the best one – Golitsyn's, haversine, flat Earth approximation (up to 100 km), great circle and Vincenty formulae. After tests made we decided to use Vincenty's direct equations [30] to compute the earthquake epicenters. An advantage of this algorithm is possibility to use reference ellipsoid in calculations and we used WGS84.

For automatic localization of events a software code based both on Golitsyn's method and Vincenty formulae was developed [Appendix 1].

29 earthquakes from the T1 group and 7 from the T2 group with clear onset of P-phases on the three components were selected and their epicenters were calculated. The results are presented in the Table 2.

Table 2. The epicentral locations of the earthquakes obtained by the single station localization code

N	Date dd.mm.yyyy	Time [hh:mm]	Latitude [deg.min]	Longitude [deg.min]	Back azimuth [degrees]	Epicentral distance [km]	Type of event
1	21.12.2015	15:38	-62.65	-60.11	95	13	T1
2	21.12.2015	21:09	-62.65	-60.15	99	11	T1
3	22.12.2015	5:23	-62.66	-60.10	101	13.5	T1
4	22.12.2015	9:25	-62.67	-60.10	104	13.5	T1
5	22.12.2015	10:55	-62.70	-60.12	121	14	T1
6	23.12.2015	2:42	-62.65	-60.11	98	13	T1
7	25.12.2015	5:47	-62.60	-60.44	312	5.5	T1
8	26.12.2015	17:24	-62.65	-60.11	97	13	T1
9	28.12.2015	19:34	-62.64	-60.10	94	13.5	T1
10	29.12.2015	7:29	-62.68	-60.06	106	16	T1
11	29.12.2015	21:05	-62.66	-60.81	264	23.5	T1
12	29.12.2015	23:47	-62.66	-60.08	102	14.5	T1
13	01.01.2016	6:58	-62.67	-60.05	103	16	T1
14	01.01.2016	18:18	-62.65	-60.07	98	15	T1
15	03.01.2016	7:38	-62.65	-60.06	98	15.5	T1
16	05.01.2016	17:16	-62.65	-60.05	94	16	T1
17	09.01.2016	4:33	-62.65	-60.11	97	13	T1
18	09.01.2016	6:18	-62.65	-60.11	96	13	T1
19	09.01.2016	6:21	-62.66	-60.10	100	13.5	T1
20	10.01.2016	1:04	-62.65	-60.09	97	14	T1
21	11.01.2016	23:45	-62.64	-60.08	92	14.5	T1
22	13.01.2016	15:58	-62.62	-60.43	300	4.5	T1
23	27.01.2016	11:02	-62.66	-60.11	100	13	T1
24	03.02.2016	8:38	-62.64	-60.06	92	15.5	T1
25	03.02.2016	21:13	-62.65	-60.09	95	14	T1
26	10.02.2016	16:20	-62.66	-60.05	100	16	T1
27	11.02.2016	17:09	-62.64	-60.07	92	15	T1
28	13.02.2016	11:11	-62.64	-60.06	91	15.5	T1
29	22.02.2016	0:52	-62.65	-60.07	96	15	T1
1	30.12.2015	5:19	-62.72	-60.93	252	31	T2
2	30.12.2015	15:58	-62.88	-61.01	231	43	T2
3	31.12.2015	12:19	-62.75	-61.07	251	38.5	T2
4	12.01.2016	18:23	-62.31	-61.01	317	49.5	T2
5	19.02.2016	9:05	-62.77	-60.89	241	31	T2
6	26.02.2016	15:30	-62.72	-60.93	252	31	T2
7	27.02.2016	8:36	-62.81	-61.23	246	48.5	T2

The next approach to locate the earthquakes was performed for stronger events recorded by other seismic stations in the region. Seismic phases related to 6 events from the T1 and T2 groups and registered by the LIVV station and the stations of AI Network were used to perform localization with DHypo minimization procedure. This software is used in the routine processing of the events in Bulgarian Seismological Data Centre [31]. The results obtained were presented in [13].

In this study a bulletin of 18 earthquakes for the period 2015–2016 was compiled and the DHypo location program was applied for earthquake locations. The bulletin comprised P wave and S wave arrival times of earthquakes recorded by the stations LIVV, ESPZ (AI), JUBA (AI) and Spanish Seismic Network deployed at Deception Island Volcano (BASE, C70, OBS, CHI) [32]. Velocity models for regions of Back Scott's Arc, Fore Scott's Arc and South Shetland Platform [10] were used for calculation of the earthquake hypocenters.

6. RESULTS AND DISCUSSION

The epicentral locations of the earthquakes listed in Table 2 were obtained applying the single station localization software code and travel-time table derived from the Back Scott's Arc velocity model [10]. The back azimuth (BAZ) and the distance to the LIVV station are given it the table together with the coordinates of the epicenters. The largest numbers of the earthquakes from T1 group have back azimuth from 90 to 100 degrees and epicentral distance in the range 11–16 km. The epicenters are clustered in eastern direction from the LIVV station and located near the east part of the south coast of Livingston Island (fig. 7).

Two events from the T1 group are located close to the station in north-western direction. The epicentral distances for these events are about 5 km and they may have glacial origin. The earthquake with largest epicentral distance of 23.5 km is situated in west direction (264 degrees back azimuth) from the LIVV station. The locations of the T1 events are mapped with red circles in the fig. 7.

Six events from the T2 group have back azimuth from 230 to 251 degrees and are located in the sea in the south-western direction from the LIVV station. The epicentral distances vary from 31 to 48 km. The epicenter of the most distant event is in Scotia Sea northwest of the station. The epicenters of the T2 earthquakes are marked with dark blue circles in the figure 7.

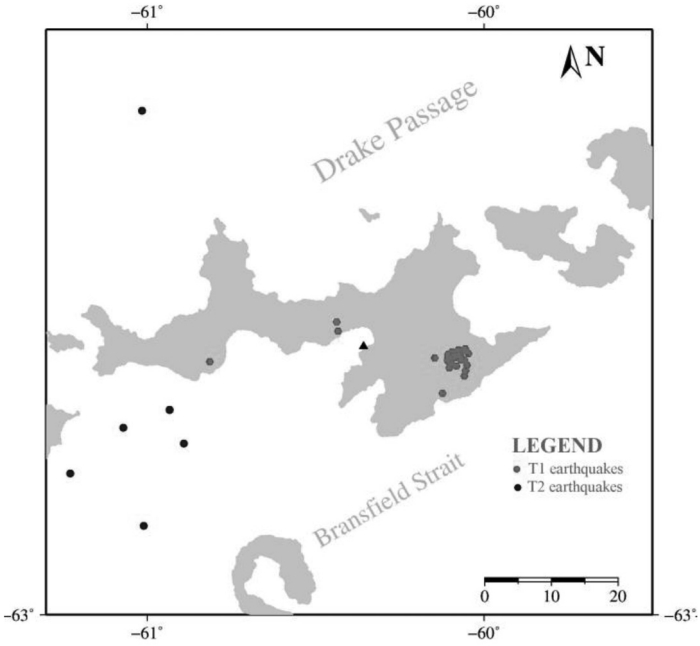

Fig. 7. Locations of the earthquakes from the T1 group mapped with red circles and from the T2 group – dark blue circles obtained by the developed code

The hypocentral estimations of 18 earthquakes included in the compiled bulletin are shown in the Appendix 2. For comparison, the locations obtained by the both procedures (Golitsyn's method and DHypo code) are shown together in the Table. The three velocity models mentioned above were used by DHypo location procedure in order the best locations to be obtained. The standard deviations of the estimations are shown as well. It can be seen that the smallest standard deviations have the epicentral estimations of the T1 group earthquakes obtained by implementing the Back Arc velocity model in DHypo procedure. The time residuals are less than 1 sec in comparison to the residuals estimated using the other two models. The best estimations of the earthquake locations from the T2 group are produced using the Fore Arc Model.

Figure 8 represents the locations of all 18 earthquakes. The T1 events are mapped with dark blue circles (by Golitsyn's method) and with light blue circles (by DHypo). The T2 events are mapped respectively with red and magenta circles.

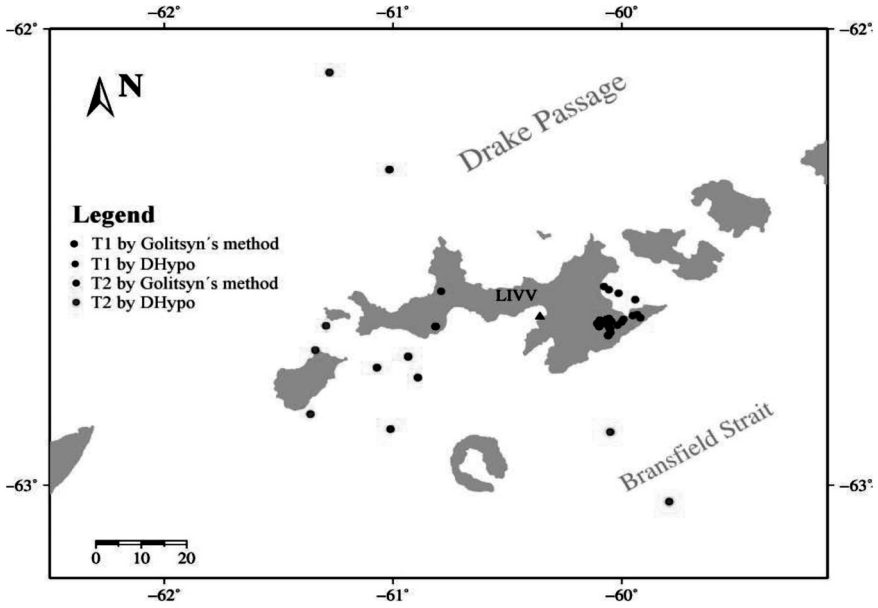

Fig. 8. Locations of the earthquakes obtained by Golitsyn's method and DHypo procedure

Main as can be seen, the earthquake locations of the events from the T1 group obtained by the both procedures are almost identical. There are significant differences in the locations for the events from the T2 group. Possible reasons are: the improper models applied; the earthquake locations are outside of the "array" of the used seismic stations.

The calculated earthquake depths are also represented in the Appendix 3. This earthquake parameter is very sensitive of velocity model applied. The results obtained suggest that the registered earthquakes are shallow with depth not more than 40 km that is typical for the seismicity in the Scott's Arc.

Magnitudes of the registered earthquakes in the season 2015–2016 are not more than 3 [13].

The most part of the all registered earthquakes from the T1 group have time difference *Ts-p* in the range 2.6–3.2 s. These earthquakes have waveforms very similar to those of the earthquakes listed in the Table 2. Taking into account these circumstances it can be supposed that their epicenters are located in eastern direction from the LIVV station near the east part of the south coast of Livingston Island (fig. 7). The large number of earthquakes realized within 73 days of deployment of LIVV station is an evidence for raised microseismic activity at this part of Livingston Island that can be related to geodynamic and volcanic processes in Bransfield Strait during the last several years [12].

7. CONCLUSIONS

Bulgarian Antarctic Broadband Seismic Station LIVV is put in operation on 19.12.2015. It is situated in close vicinity of Bulgarian Antarctic Base „St. Kliment Ohridski" on Livingston Island. During the first period of operation in the astral summer 2015–2016 about 200 earthquakes are registered. The estimated performance of the installed seismic equipment and the number of registered seismic events show the ability of LIVV station to record events of different origin and epicentral distance. 36 events with clear P wave onsets are located using code based on Golitsyn's method and Vincenty formulae. DHypo location program with appropriate velocity models is used to perform locations of 18 events registered by Bulgarian station LIVV, AI seismic stations ESPZ and JUBA and Spanish network at Deception Island Volcano (BASE, C70, OBS, CHI). The epicentral estimations of the local earthquakes (epicentral distance less than 16 km) calculated by the both procedures are almost equals. Most epicenters are clustered in the eastern part of the Livingston Island which show higher microseismicity related to geodynamic processes in the region of Back Scott's Arc. Several events are generated in the western direction from the station LIVV within a distance range from 31 to 48 km and could be related to the seismicity realized in the region of Fore Scott's Arc.

Long term monitoring of the seismicity in the region will provide large amount of data for detailed investigation of the crustal structure of Livingston Island and surroundings and further insight into the complex and unique system of Scott's Arc.

Acknowledgements. The presented paper is prepared as a result of the implementation of the project DFNI I02/11/2014 "Creating an information base for exploration of seismicity and Earth structure of Livingston island and surroundings by complex research in the Bulgarian Arctic Base area" supported by the Science Research Fund to Bulgarian Ministry of Education and Science.

APPENDICES

APPENDIX 1

```
from __future__ import division
import numpy as np
import datetime
from math import atan
from math import atan2
from math import cos
from math import radians
from math import sin
from math import sqrt
from math import tan
import math
import sys
```

```
# Station LIVV coordinates
LIVV_Lat = -62.636
LIVV_Lon = -60.3580
# WGS84
a = 6378.137
b = 6356.7523142
flt = 0.00335281066475   # flt = 1/298.257223563

def vincenty(LatSt, LongSt, alphaStEp, s):
   latstRad = math.radians(float(LatSt))
   lonstRad = math.radians(float(LongSt))
   azimRad = math.radians(float(alphaStEp))
   tanU1 = (1.0 - float(flt))*math.tan(latstRad)
   U1 = math.atan(tanU1)                    # in Radians
   tanSigma1 = tanU1 / math.cos(azimRad)
   sigma1 = math.atan(tanSigma1)            # in Radians
   sinAlpha = math.cos(U1) * math.sin(azimRad)
   cosSQalpha = 1.0 - sinAlpha * sinAlpha
   uSQ =  (cosSQalpha *(a * a - b * b) )/ (b * b)
   A = 1 + (uSQ / 16384) * (4096 + uSQ * (-768 + uSQ * (320 - 175 * uSQ)))
   B = (uSQ / 1024) * (256 + uSQ * (-128 + uSQ * (74 - 47 * uSQ)))
   sigma = (float(s) / (float(b) * float(A)))   # sigma initial value
   NewSigma = sigma
   LastSigma = 2.0 * sigma
   while (abs(NewSigma - LastSigma) > 1.0e-12):
      twoSigma_m = 2.0 * sigma1 + NewSigma
      deltaSigma = B * math.sin(LastSigma) * (math. cos(twoSigma_m) + (B/4) * \
         (math.cos(NewSigma) * (-1 + 2 * math.pow(math.cos(twoSigma_m) , 2)) \
         - (B/6) * math.cos(twoSigma_m) * (-3 + 4 * \
         math.pow(math.sin(NewSigma),2)) * \
         (-3 + 4 * math.pow(math.cos(twoSigma_m),2))))
      LastSigma = NewSigma
      NewSigma = (float(s) / (float(b) * float(A))) + deltaSigma
   sigma = NewSigma
   M = math.sin(U1) * math.cos(sigma) + math.cos(U1) * math.sin(sigma) * \
      math.cos(azimRad)
   N = (1.0 - float(flt)) * math.sqrt( math.pow(sinAlpha,2) + \
      math.pow((math.sin(U1) * math.sin(sigma) - math.cos(U1) * \
      math.cos(sigma) * math.cos(azimRad)),2))
   latEpRad = math.atan2(M,N)               # in Radians
   P = math.sin(sigma) * math.sin(azimRad)
   Q = math.cos(U1) * math.cos(sigma) - math.sin(U1) * math.sin(sigma) * \
      math.cos(azimRad)
   lonEpTMP = math.atan2(P,Q)               # in Radians
   C = (float(flt)/16) * cosSQalpha * (4 + float(flt) * (4 - 3 * cosSQalpha))
   L = lonEpTMP - (1.0 - C) * float(flt) * sinAlpha * \
      (sigma + C * math.sin(sigma) * (math.cos(twoSigma_m) + \
      C * math.cos(sigma) * (-1.0 + 2.0 * math.pow(math.cos(twoSigma_m),2))))
   lonEpRad = L + lonstRad                  # in Radians
   LatEp = math.degrees(latEpRad)
   LongEp = math.degrees(lonEpRad)
   return {'EpLong' : LongEp, 'EpLat' : LatEp} #'alphaEpStaaz': ne se presmqta za sega

def compute_baz_Golitcin(An1,Ae1,Az1):
   azim = math.fabs(math.degrees(math.atan(int(Ae1)/int(An1))))
   print "Initial azimuth", azim
   if any( [
      all( [An1>0, Ae1>0, Az1<0] ),
      all( [An1<0, Ae1<0, Az1>0] )
```

```
    ] ):
      baz = azim
      print "Case azs=az, azimuth is:", baz
   elif any( [
       all( [An1>0, Ae1<0, Az1>0] ),
       all( [An1<0, Ae1>0, Az1<0] )
    ] ):
      baz = 180-azim
      print "Case azs=180-az, azimuth is:", baz
   elif any( [
       all( [An1>0, Ae1>0, Az1>0] ),
       all( [An1<0, Ae1<0, Az1<0] )
    ] ):
      baz = 180+azim
      print "Case azs=180+az, azimuth is:", baz
   elif any( [
       all( [An1>0, Ae1<0, Az1<0] ),
       all( [An1<0, Ae1>0, Az1>0] )
    ] ):
      baz = 360 - azim
      print "Case azs=360-az, azimuth is:", baz
   return baz

def hodograf(tsp):
   travelTimeSP = {}
   with open('travelTimeSP.text_py_mod', 'r') as f:
      for line in f:
         splitLine = line.split()
         travelTimeSP[splitLine[0]] = ",".join(splitLine[1:])
      if travelTimeSP.has_key(tsp):
         return travelTimeSP[tsp]
      else:
         new_tsp = min(travelTimeSP.keys(), key=lambda k:
abs(float(tsp)-float(k)))
         return travelTimeSP[new_tsp]
###
if len(sys.argv) > 1:
   f=open(sys.argv[1],'r')
else:
   print ""
   print "File with initial data is missing!"
   print ""
   print "\t Usage: python",sys.argv[0]," < filename >"
   print ""
   sys.exit(0)

row=f.readlines()
f.close()
csvfile=open('EQ_epicenters.csv','w')
forgmtfile = open('forGMT_plot.dat','w')
for i in row:
   dt,aan,aae,aaz,origind=i.split('\t')  # See README_oneStaEQLoc for more info
   wreme = datetime.datetime.strptime(str(origind),"%m.%d.%Y %H:%M ")
   An = int(aan)
   Ae = int(aae)
   Az = int(aaz)
   print "######### Start of the event processing! #########"
   print "Date, An,Ae,Az, S-P", wreme, An, Ae, Az, dt
   azimuth = compute_baz_Golitcin(An,Ae,Az)
 distancekm = hodograf(dt)
```

```
    # Computation of coordinates
    Ev_coord = vincenty(LIVV_Lat, LIVV_Lon, azimuth,  distancekm)
    print
    print "Epicenter location, Distance from hodograph:", Ev_coord['EpLong'], \
          Ev_coord['EpLat'], distancekm
    csvfile.write("{0};{1};{2};{3};{4}\n".format( wreme, Ev_coord['EpLong'], \
          Ev_coord['EpLat'], azimuth, distancekm))
    forgmtfile.write("{0}\t{1}\n".format(Ev_coord['EpLong'], Ev_coord['EpLat']))
    print "************ End of the event procesing ************"
    print " "
csvfile.close()
forgmtfile.close()
```

APPENDIX 2

Table A. The hypocentral estimations of 18 earthquakes included in the compiled bulletin obtained by Golitsyn's method and Dhypo procedure with SSP velocity model

	Locations by Golitsyn's method					Locations obtained by Dhypo procedure			
	SSP velocity model					SSP velocity model			
N	Date [dd.mm.yy]	Time [hh:mm]	Lat [deg. min]	Long [deg. min]	Type of event	Lat [deg. min]	Long [deg. min]	Depth [km]	Sd
1	28.12.2015	19:34	-62.64	-60.10	T1	-62.63	-60.08	15	0.5
2	29.12.2015	7:29	-62.68	-60.06	T1	-62.73	-60.31	7.5	0.48
3	29.12.2015	21:05	-62.66	-60.81	T1	-62.65	-60.79	6.6	0.06
4	03.01.2016	7:38	-62.65	-60.06	T1	-62.75	-60.21	3	0.15
5	05.01.2016	17:16	-62.65	-60.05	T1	-62.70	-59.81	4.3	0.2
6	09.01.2016	4:33	-62.65	-60.11	T1	-62.74	-60.28	4	0.07
7	09.01.2016	6:21	-62.66	-60.10	T1	-62.74	-60.25	2	0.1
8	03.02.2016	8:38	-62.64	-60.06	T1	-62.66	-60.23	14.2	0.02
9	03.02.2016	21:13	-62.65	-60.09	T1	-62.74	-60.23	2	0.07
10	10.02.2016	16:20	-62.66	-60.05	T1	-62.75	-60.16	2	0.17
11	11.02.2016	17:09	-62.64	-60.07	T1	-62.62	-59.94	15	0.63
12	22.02.2016	0:52	-62.65	-60.07	T1	-62.70	-60.21	10.7	0.1
1	30.12.2015	5:19	-62.72	-60.93	T2	-62.89	-60.05	8.5	0.09
2	30.12.2015	15:58	-62.88	-61.01	T2	-62.85	-61.36	36.2	0.19
3	31.12.2015	12:19	-62.75	-61.07	T2	-62.97	-60.01	8.1	0.6
4	12.01.2016	18:23	-62.31	-61.01	T2	-62.10	-61.28	17.1	0.21
5	19.02.2016	9:05	-62.77	-60.89	T2	-62.66	-61.29	2	0.3
6	26.02.2016	15:30	-62.72	-60.93	T2	-62.71	-61.34	2.1	0.24

Table B. The hypocentral estimations of 18 earthquakes included in the compiled bulletin obtained by Dhypo procedure with back arc and fore arc velocity model

	Back Scott's Arc velocity model				Fore Scott's Arc velocity model			
N	Lat [deg.min]	Long [deg.min]	Depth [km]	Sd	Lat [deg.min]	Long [deg. min]	Depth [km]	Sd
1	-62.65	-60.00	2.4	0.19	-62.65	-60.04	5.4	0.22
2	-62.67	-60.05	2.8	0.51	-62.72	-60.15	2	0.42
3	-62.58	-60.79	2	0.12	-62.69	-60.52	10	0.39
4	-62.64	-59.92	3.6	0.29	-62.61	-59.99	10	0.3
5	-62.63	-59.93	9.1	0.21	-62.61	-59.94	10	0.33
6	-62.65	-60.02	3.8	0.2	-62.67	-60.08	5.1	0.23
7	-62.63	-59.95	3.6	0.23	-62.62	-60.07	8.2	0.24
8	-62.57	-60.08	18.1	0	-62.58	-60.13	19.5	0.01
9	-62.64	-59.99	3.4	0.22	-62.69	-60.07	2	0.22
10	-62.60	-59.94	12.5	0.31	-62.61	-59.96	10	0.3
11	-62.58	-60.06	16.8	0.18	-62.60	-59.97	10	0.25
12	-62.58	-60.01	15	0.1	-62.60	-60.03	15.2	0.1
1	-62.97	-59.68	3.9	0.11	-62.94	-59.81	2	0.08
2	-62.83	-61.73	10	0.14	-62.81	-61.73	10	0.15
3	-62.72	-61.33	26.6	0.46	-63.04	-59.79	2	0.53
4	-62.06	-61.34	2	0.34	-62.08	-61.30	0.9	0.18
5	-62.66	-61.29	2	0.3	-62.66	-61.29	2	0.3
6	-62.71	-61.34	2.1	0.24	-62.81	-60.39	5	0

REFERENCES

[1] Gutenberg, B., Richter, C.F. Seismicity of the earth and associated phenomena. Princeton University Press, 1954.

[2] Richter, C. F. Freeman. San Francisco, 1958.

[3] Kaminuma, K. *J. of Indian Geophys. Union*, 2006, **10**, 15.

[4] Kaminuma, K. *Antarct. Geosc.*, 1995, **8**, 35.

[5] Kaminuma, K., Ishida, M. *Antarct. Rec.*, 1971, **42**, 53.

[6] Adams, R.D. *Antarct. Geol. and Geophys.*, 1972, 495.

[7] Adams, R.D. *Antarct. Geosc.*, 1982, 955.

[8] Grad, M. H., H. Shiobara, T. Janik, A., Guterch, H. Shimamura. *Geophys. J. Int.*, 1997, **130,** 506.

[9] Pelayo, A. M., Wiens, D. A. *J. of Geoph. Res.*, 1989, **94(B6)**, 7293.

[10] Robertson Maurice, S. D., D. A. Wiens, P. J. Shore, E. Vera, L. M. Dorman. *J. of Geoph. Res.*, 2003, **108(B10)**, 2461.

[11] Carmona, E., Almendros, J., Martín, R., Cortés, G., Alguacil, G., Moreno, J. *Annals of Geoph.*, 2014, **57(3)**.

[12] Almendros, J., Carmona, E.,Jiménez, V., Díaz-Moreno, A., Lorenzo, F. *Geoph. Res. Lett.*, 2018, **45**, 4788.

[13] Dimitrova, L., G. Georgieva**,** R. Raykova, D. Dimitrov, V. Gurev, D. Solakov, I. Georgiev, P. Raykova, V. Protopopova, I. Aleksandrova, M. Popova. *Compt. Rend. De l'Acad. Bulg. Des Sc.*, 2017, **70**, 1310.

[14] Martínez Arévalo, C., F. Mancilla, J. Almendros, J. L. Aznarte, G. Alguacil. *Abstract from EGU General Assembly 2009,* Vienna, Austria*,* 2009, 13362.
[15] Rangelov, B. *Yearbook of the University of Mining and Geology St. Ivan Rilski",* 2002, **45**, 117. (in Bulgarian).
[16] Backer, P. F. *J. Geol. Soc. Lon.*, 1982, **139**, 787.
[17] Smellie, J. L., X. J. Pankhurst, M. R. A. Thomson, R. E. S. Davies. *VI. Stratigraphy, Geochemistry and Evolution, British Antarctic Survey Scientific Reports*, 1984, **87**, 85.
[18] Kamenov, B. Bulgarian Antarctic Research – a synthesis, 2015, University Press "St. Kliment Ohridski", 2015.
[19] Keller, R. A., M. R. Fisk, W. M. White, K. Birkenmajer. *Earth Planet. Sci. Lett.*, 1992, **111**, 287.
[20] Smellie, J. L. *Antarc. Sc.*, 2001, **13**, 188.
[21] Cande, S. C., Herron, E. M., Hall, B. R. *Earth Planet. Sci. Lett.*, 1982, **57**, 63.
[22] Larter, R. D., Baker, P. F.. *J. of Geoph. Res. Atmosph.*, 1991, **96(B12)**, 19583.
[23] Ivanov, L., Antarctica: Livingston Island and Greenwich, Robert, Snow and Smith Islands. 2010, Scale 1:120000 topographic map 2nd ed. Troyan: Manfred Wörner Foundation.
[24] McNamara, D., Buland, R. *Bull. of Seism. Soc. of America*, 2004, **94(4)**, 1517.
[25] Peterson, J. *USGS Numbered Series*, *Open-File Report*, 1993, **93-322,** 1517.
[26] http://dx.doi.org/doi:10.7914/SN/AI
[27] http://ds.iris.edu
[28] Golitsyn, B.B. Selected works (Vol. 2), Moscow, Science Acad. USSR, 490 (in Russian).
[29] Christoskov, L. Seismology (Part II), Sofia, University "St. Kl. Ohridski", 455 pp. (in Bulgarian).
[30] Vincenty, T. *Surv. Rev. XXIII*, 1975a, **176**, 88.
[31] Solakov, D. *Bulg. Geophys. J.,* 1993, **19(1)**, 56.
[32] http://dx.doi.org/doi:10.4225/15/5ac5681e2f528